

in which small differences appear when compared with low-spin six-coordinate iron(II) porphyrins such as $\text{Fe}(\text{Pip})_2(\text{TPP})^{23}$ and $\text{Fe}(\text{THT})_2(\text{TPP})\text{-THT}^{24}$ (Table IV). These small changes that appear in the core of $[\text{Fe}(\text{TPP})]^-$ have been interpreted as being due to a small contribution of a spin-coupled iron(II) porphyrin radical anion, $[\text{Fe}^{\text{II}}(\text{TPP})]^-$.²² A minor contribution of a spin-coupled cobalt(II) porphyrin radical anion could also be present in $[\text{Co}(\text{TPP})]^-$ by occupation of the lowest unoccupied molecular orbital (LUMO) of e_g symmetry. The porphyrin LUMO is antibonding with respect to $\text{N}-\text{C}_\alpha$ and bonding relative to $\text{C}_\alpha-\text{C}_\beta$ and $\text{C}_\beta-\text{C}_\beta$. However, in such a spin-coupled cobalt(II) radical porphyrin anion the orbital containing the unpaired electron present in the low-spin cobalt(II) center should have the same symmetry as the porphyrin LUMO. Or, this is in conflict with the well-known $(d_{z^2})^1$ configuration of low-spin cobalt(II) in cobalt(II) porphyrins. Consequently, it is more reasonable to assume that the small changes that appear in the $(\text{N}-\text{C}_\alpha)_{\text{av}}$, $(\text{C}_\alpha-\text{C}_\beta)_{\text{av}}$, and $(\text{C}_\beta-\text{C}_\beta)_{\text{av}}$ bond lengths are due to enhanced back-donation of the electron-rich Co(I) center toward the porphyrin II system when compared with the back-donation of the nickel center in Nickel(II) porphyrins. In this case, the occupied

$(d_{xz})^2$ and $(d_{yz})^2$ cobalt orbitals have the symmetry of the porphyrin LUMO. Furthermore, this enhanced back-donation with the concomitant changes in some bond lengths of the porphyrin skeleton is most probably also indirectly responsible for the nonobservation of HOARD's rule in $[\text{Co}(\text{TPP})]^-$.¹⁶ In summary, the structure of $[\text{Co}(\text{TPP})]^-$ is consistent with a cobalt(I) porphyrin formulation, $[\text{Co}^{\text{I}}(\text{TPP})]^-$, with a strong back-donation from the metal into the porphyrin II system.

Table IV gives the average bond distances and angles found within the complex cations, $[\text{K}\subset 222]^+$. As usual, the potassium ion is completely enclosed by the macrobicyclic ligand. The average K-O and K-N distances are similar to those found elsewhere.²⁵ The Cl^- anions and the water molecule present in the asymmetric unit are arranged in centrosymmetric, $\text{Cl}-\text{HOH}-\text{Cl}'-\text{HOH}-\text{Cl}$ units in which three chloride ions are linked together via two hydrogen-bonded water molecules. The two $\text{Cl}-\text{O}$ and $\text{Cl}'-\text{O}$ distances are 3.29 and 3.27 Å, respectively, and the $\text{Cl}-\text{OH}_2-\text{Cl}'$ angle is 118°. All the Co-Cl and Co-OH₂ separations are larger than 8.75 and 10.14 Å, respectively.

Registry No. 1, 91209-58-4; $\text{Co}^{\text{III}}(\text{TPP})\text{Cl}$, 60166-10-1; $[\text{K}\subset 222]$ 2-methyl-2-propanethiolate, 91209-59-5.

Supplementary Material Available: Listings of least-squares planes, H atom positional parameters, general temperature factors of all anisotropic atoms, and observed and calculated structure factors (30 pages). Ordering information is given on any current masthead page.

- (21) Haller, K. J.; Scheidt, W. R.; Reed, C. A., to be submitted for publication.
 (22) Reed, C. A. *Adv. Chem. Ser.* **1982**, No. 201.
 (23) Radonovich, L. J.; Bloom, A.; Hoard, J. L. *J. Am. Chem. Soc.* **1972**, *94*, 2073-2078.
 (24) Mashiko, T.; Reed, C. A.; Haller, K. J.; Kastner, M. E.; Scheidt, W. R. *J. Am. Chem. Soc.* **1981**, *103*, 5758-5767.

- (25) Moras, D.; Weiss, R. *Acta Crystallogr., Sect. B: Struct. Crystallogr. Cryst. Chem.* **1973**, *29*, 396-399.

Contribution from the Departments of Chemistry, University of Cincinnati, Cincinnati, Ohio 45221, and University of Oklahoma, Norman, Oklahoma 73019

Synthesis and Characterization of Technetium(V) 8-Quinolinolates. X-ray Crystal Structure of *cis*-Chlorobis(2-methyl-8-quinolinolato)oxotechnetium(V)

BRUCE E. WILCOX,¹ MARY JANE HEEG,² and EDWARD DEUTSCH*¹

Received December 13, 1983

Technetium(V) complexes of 8-quinolinolates of the form TcOL_2X (L = 8-quinolinolate and its 5,7-dichloro, 5,7-dibromo, 5-nitro, and 2-methyl derivatives; X = Cl, Br) have been synthesized and characterized. These neutral species precipitate from methanol after reaction of the quinolinolate ligand with TcOX_4^- . HPLC analyses of the complexes show that the halide ligand of *cis*- $\text{TcO}(\text{8-quinolinolate})_2\text{X}$ is susceptible to solvolysis in methanol, forming what is believed to be $\text{TcO-L}_2(\text{OCH}_3)$; when X is Cl, the specific first-order rate constant governing this process is $1 \times 10^{-4} \text{ s}^{-1}$ (25 °C, no ionic strength, in methanol). A single-crystal X-ray structure determination shows that the chlorobis(2-methyl-8-quinolinolato)oxotechnetium(V) complex, $\text{TcO}(\text{CH}_3\text{C}_9\text{H}_7\text{NO})_2\text{Cl}$, formula weight 467, has a distorted-octahedral coordination geometry, with the chloro and oxo ligands in a *cis* configuration. A oxo-induced structural trans effect characteristic of $\text{M}=\text{O}$ moieties is manifested in a lengthening of the Tc-O bond trans to the yl oxygen and a displacement of the Tc atom out of the mean equatorial plane. This complex crystallizes in the triclinic centrosymmetric space group $P\bar{1}$ with $a = 7.693$ (2) Å, $b = 9.337$ (2) Å, $c = 12.739$ (3) Å, $\alpha = 86.52$ (2)°, $\beta = 85.99$ (2)°, $\gamma = 84.12$ (2)°, and $V = 907$ (2) Å³, with $Z = 2$, for 2882 observed reflections with $I_o \geq 2\sigma(I)$. Structural aspects of metal complexes containing 8-quinolinolate ligands are discussed.

Introduction

Complexes formed from the short-lived isotope $^{99\text{m}}\text{Tc}$ ($t_{1/2} = 6$ h) are widely used in nuclear medicine as imaging agents because of the ideal nuclear properties of $^{99\text{m}}\text{Tc}$.³ Adducts of 8-quinolinol and technetium-99m have been reported to have high brain uptake in laboratory animals,⁴ but the chemical

identities of the moieties leading to this uptake are not known. In order to obtain information about the possible composition and nature of these $^{99\text{m}}\text{Tc}$ moieties, we have undertaken a study of 8-quinolinol technetium complexes using macroscopic amounts of the relatively stable isotope ^{99}Tc ($t_{1/2} = 2.1 \times 10^5$ years). It is hoped that this study will eventually lead to the development and in vivo evaluation of well-characterized 8-quinolinol $^{99\text{m}}\text{Tc}$ imaging agents.

(1) University of Cincinnati.
 (2) University of Oklahoma.
 (3) Deutsch, E.; Libson, K.; Jurisson, S.; Lindoy, L. F. *Prog. Inorg. Chem.* **1983**, *30*.

(4) Loberg, M. D.; Corder, E. H.; Fields, A. T.; Callery, P. S. *J. Nucl. Med.* **1979**, *20*, 1181.

A variety of transition metals form complexes with 8-quinolinol, but no well-defined technetium complexes of this ligand have been reported.³ This historical situation results in large part from the lack, until recently, of convenient starting materials for the synthesis of technetium complexes, exacerbated by the intricate chemistry of technetium and the underdeveloped state of this field.³ Thus, for many years the only practicable starting material for the synthesis of technetium complexes was pertechnetate, $\text{Tc}^{\text{VII}}\text{O}_4^-$, and the reaction of pertechnetate with 8-quinolinol in aqueous HCl leads to a complicated mixture of complexes containing technetium in oxidation states lower than VII.⁵ However, the technetium(V) complexes TcOX_4^- ($X = \text{Cl}, \text{Br}$) have been recently characterized and shown to be convenient starting materials for the synthesis of a variety of technetium(V) complexes.^{6,7} These synthetic reactions involve simple displacement of the relatively labile halides by the ligand of interest. In this paper we report on the synthesis, characterization, and reactivity of 8-quinolinolate complexes of technetium(V) prepared by substitution of the ligand onto TcOCl_4^- and TcOBr_4^- .

Experimental Section

General Procedures. Technetium-99 emits a low-energy (0.292 MeV) β particle with a half-life of 2.12×10^5 years. When this material is handled in milligram amounts, it does not present a serious health hazard since common laboratory materials provide adequate shielding. Bremsstrahlung is not a significant problem due to the low energy of the β -particle emission, but normal radiation safety procedures must be used at all times to prevent contamination.

All common laboratory chemicals used were of reagent grade. $[\text{Bu}_4\text{N}]\text{TcOCl}_4$ ^{6a} and $[\text{Bu}_4\text{N}]\text{TcOBr}_4$ ⁷ (where $\text{Bu} = n\text{-C}_4\text{H}_9$) were prepared as reported. 8-Quinolinol (Hox) (Eastman) was recrystallized once before use. 5,7-Dichloro-8-quinolinol (HoxCl_2), 5,7-dibromo-8-quinolinol (HoxBr_2), 5-nitro-8-quinolinol (HoxNO_2), and 8-hydroxy-2-methylquinoline (HoxMe) (Aldrich) were used as received. HPLC mobile phases were prepared from triply distilled water and HPLC grade methanol (Fisher). All mobile phases and samples were filtered through 0.45- μm Nylon-66 filters (Rainin). HPLC analyses were performed on a Beckman Model 334 gradient liquid chromatograph with a 254-nm UV detector using a C_8 reversed-phase column (Jones) with a pellicular C_8 precolumn (Anspec). IR spectra were recorded on a Perkin-Elmer 599 grating spectrometer using KBr pellets. UV-vis spectra were recorded on a Cary 210 spectrophotometer at ambient temperature. Microanalyses were performed by Guelph Laboratories, Ltd., Guelph, Ontario, Canada.

Preparation of Complexes. All complexes were synthesized by a procedure detailed here for the 8-quinolinol derivative, $\text{TcO}(\text{ox})_2\text{Cl}$. To a stirred solution of 215 mg (0.431 mmol) of $[\text{Bu}_4\text{N}]\text{TcOCl}_4$ in approximately 25 mL of methanol was slowly added a solution of 167 mg (1.15 mmol) of Hox in approximately 15 mL of methanol. The reaction solution turned immediately from the light green color of the TcOCl_4^- to an intense red-brown color. After 3 h a dark red-brown precipitate was collected by filtration and rinsed with a small portion of methanol. The yield based on $\text{TcO}(\text{ox})_2\text{Cl} \cdot \text{H}_2\text{O}$ was 88%. Allowing the reaction mixture to stand for 2 days yielded an additional small amount of solid product. Anal. Calcd for $\text{TcO}(\text{ox})_2\text{Cl} \cdot \text{H}_2\text{O}$: C, 47.34; H, 3.09; N, 6.13; Cl, 7.76. Found: C, 47.74; H, 2.71; N, 6.20; Cl, 8.03. The $\text{TcO}(\text{ox})_2\text{Br}$ analogue can be similarly prepared from $[\text{Bu}_4\text{N}]\text{TcOBr}_4$.

HPLC Studies. Sample solutions were prepared by dissolution of the solid material in methanol followed by filtration through a 0.45- μm Nylon-66 disposable unit. Chromatographic conditions: mobile phase, 58/42 (v/v) methanol/water with 8 mM phosphate buffer at pH 7; flow rate 1.5 mL/min; injection volume 10–20 μL ; detector 254-nm UV with 0.04 AUFS. All mobile phases were degassed by sonication before use.

Table I. UV-Vis and IR Spectral Parameters for 8-Quinolinolate Complexes of Technetium(V)^a

complex ^b	λ_{max} (ϵ) ^c		$\nu_{\text{Tc=O}}$
	nm	$\text{M}^{-1} \text{cm}^{-1}$	
$\text{TcO}(\text{ox})_2\text{Cl}$	404 (9600)	251 (60 000)	945
$\text{TcO}(\text{ox})_2\text{Br}$	403 (8200)	251 (50 000)	970
$\text{TcO}(\text{oxCl}_2)_2\text{Cl}$	419 (1400)	259 (10 900)	945
$\text{TcO}(\text{oxBr}_2)_2\text{Cl}$	421 (1300)	263 (8000)	960
$\text{TcO}(\text{oxMe})_2\text{Cl}$	403 (5800)	254 (43 000)	945
$\text{TcO}(\text{oxNO}_2)_2\text{Cl}$	425 (15 000)	248 (26 000)	970

^a λ_{max} in nm; ϵ in $\text{M}^{-1} \text{cm}^{-1}$; ν in cm^{-1} . ^b Ligand acronyms defined in Experimental Section. ^c Dichloromethane solutions.

X-ray Characterization of Chlorobis(2-methyl-8-quinolinolato)-oxotechnetium(V), $\text{TcO}(\text{oxMe})_2\text{Cl}$. The title compound crystallizes as deep red parallelepipeds from dichloromethane by slow evaporation. A fragment of approximate size $0.09 \times 0.13 \times 0.25$ mm was selected for data collection on a CAD-4 automated diffractometer using Mo $K\alpha$ radiation passed through a graphite monochromator. A total of 3648 reflections were collected at ambient temperature in the sphere $3^\circ \leq 2\theta \leq 52^\circ$. After averaging, 2882 observed reflections were obtained where $I_o \geq 2\sigma(I)$. The unit cell parameters resulting from least-squares calculations on 25 high-angle reflections were $a = 7.693$ (2) \AA , $b = 9.337$ (2) \AA , $c = 12.739$ (3) \AA , $\alpha = 86.52$ (2)°, $\beta = 85.99$ (2)°, $\gamma = 84.12$ (2)°, and $V = 907$ (2) \AA^3 . Other details of data collection: scan method θ - 2θ ; scan rate variable up to 45 s/scan; scan range calculated as $0.80 + 0.20 \tan \theta$ with 25% extensions on each side for backgrounds. Three peaks were monitored for intensity fluctuations every 2 h of X-ray time and were observed to fluctuate 1% over the entire data collection. Three orientation standards were centered after every 200 observations. Absorption corrections were applied with $\mu(\text{Mo } K\alpha) = 9.03 \text{ cm}^{-1}$ and transmission coefficients varying from 0.85 to 0.95. The calculated density was 1.709 g cm^{-3} with $Z = 2$.

The centrosymmetric space group $P\bar{1}$ gave satisfactory refinement. Placement of the heavy atoms Tc and Cl resulted from a Patterson synthesis calculation.⁸ All other non-hydrogen atoms were located from a series of Fourier maps and were refined anisotropically. Hydrogen atoms were placed at observed positions and held invariant while their isotropic temperature parameters were assigned a single variable and refined. Full-matrix least-squares refinement of all observed reflections yielded $R = 0.035$ and $R_w = 0.038$.⁹ The maximum shift in the last cycle was 0.04σ , the number of variables was 245, and the number of observations was 2882. In the final difference map the largest peak represented $<0.5 \text{ e } \text{\AA}^{-3}$ in the vicinity of a methyl group. Neutral-atom scattering factors and corrections for anomalous dispersion were obtained from ref 10.

Results

Synthesis and Characterization. The utility of TcOX_4^- as starting material for the preparation of Tc(V) complexes has been demonstrated previously for both $X = \text{Cl}^{11-14}$ and $X = \text{Br}$.⁷ In this study, solid products were readily obtained by displacement of the halide ligands of TcOX_4^- in methanol with the 8-quinolinolate (ox) ligand and some of its derivatives, i.e., 5,7-dichloro-8-quinolinolate (oxCl_2), 5,7-dibromo-8-quinolinolate (oxBr_2), 2-methyl-8-quinolinolate (oxMe), and 5-nitro-8-quinolinolate (oxNO_2). The products are generally soluble in organic solvents such as dichloromethane, chloroform, and toluene and are only slightly soluble in methanol.

- (5) (a) Rulfs, C. L. *CRC Crit. Rev. Anal. Chem.* **1970**, *1*, 335. (b) Rajec, P.; Mikulaj, V. *Radiochem. Radioanal. Lett.* **1975**, *17*, 375.
 (6) (a) Davison, A.; Trop, H. S.; DePamphilis, B. V.; Jones, A. G. *Inorg. Synth.* **1982**, *21*, 160. (b) Davison, A.; Jones, A. G. *Int. J. Appl. Radiat. Isot.* **1982**, *33*, 875.
 (7) Thomas, R. W.; Davison, A.; Trop, H. S.; Deutsch, E. *Inorg. Chem.* **1980**, *19*, 2840.

- (8) All computations were performed with local modifications of the programs of SHELX-76: Sheldrick, G. M., University Chemical Laboratory, Cambridge, England, 1976.
 (9) $R_w = [\sum w(|F_o| - |F_c|)^2 / \sum w F_o^2]^{1/2}$.
 (10) "International Tables for Crystallography"; Kynoch Press: Birmingham, England, 1974; Vol. 4.
 (11) Jurisson, S.; Lindoy, L. F.; Dancy, K. P.; McPartlin, M.; Tasker, P. A.; Uppal, D. K.; Deutsch, E. *Inorg. Chem.* **1984**, *23*, 227.
 (12) Trop, H.; Jones, A.; Davison, A. *Inorg. Chem.* **1980**, *19*, 1993.
 (13) Davison, A.; Orvig, C.; Trop, H. S.; Sohn, M.; DePamphilis, B. V.; Jones, A. G. *Inorg. Chem.* **1980**, *19*, 1988.
 (14) Bandoli, G.; Mazzi, U.; Clemente, D. A. f. Roncari, E. *J. Chem. Soc., Dalton Trans.* **1982**, 2455.

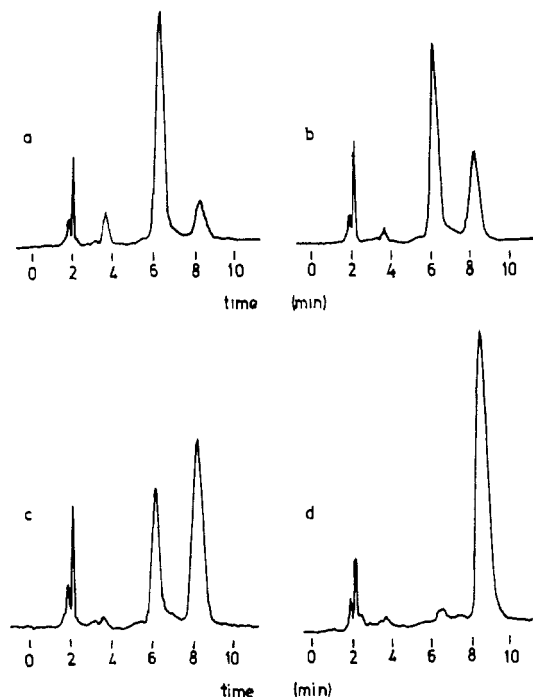


Figure 1. HPLC chromatograms resulting from successive injections of $\text{TcO}(\text{ox})_2\text{Cl}$ in methanol. Time of sample injection: (a) 25 min; (b) 77 min; (c) 180 min; (d) 18 h (post solution preparation).

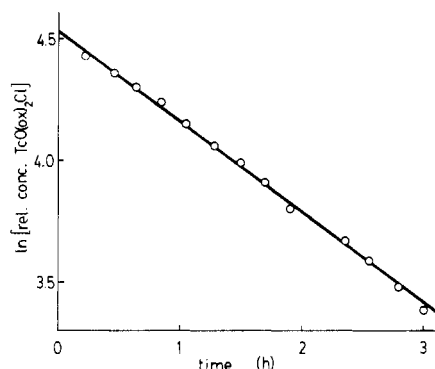


Figure 2. First-order kinetic plot for the methanolysis of $\text{TcO}(\text{ox})_2\text{Cl}$. Only the areas of the 6.4- and 8.5-min peaks were considered (see Figure 1). Relative concentration equals the area of the 6.4-min peak expressed as a percent of total peak area (corrected to $t = 18$ h). This treatment neglects spurious peaks in the chromatogram and corrects for small variations in the injection volume.

The complex of oxNO_2 is more soluble in methanol than the others.

Table I lists the UV-vis and IR spectral parameters for various 8-quinolinolato complexes. The UV-vis spectra of all of the complexes are quite similar, with the visible absorption maxima occurring at longer wavelengths for those species with electron-withdrawing groups on the backbone of the ligand. Solutions of these complexes are generally red-brown in color, the nitro derivative being more orange in color than the others. The salient infrared parameter for these complexes is the strong absorption between 945 and 970 cm^{-1} assignable to the $\text{Tc}=\text{O}$ stretch of the TcO^{3+} core.³

HPLC analyses of methanol solutions of $\text{TcO}(\text{ox})_2\text{Cl}$ and $\text{TcO}(\text{ox})_2\text{Br}$ afforded some information on the reactivity of these species. Figure 1 shows chromatograms resulting from successive injections of the same methanol solution of $\text{TcO}(\text{ox})_2\text{Cl}$ at various times after preparation of the solution. The peak at retention time 6.4 min decreases with time while the peak at retention time 8.5 min correspondingly increases with time. The time dependence of the peak areas shows that the

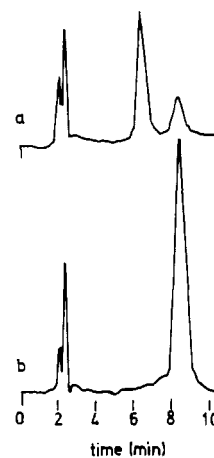


Figure 3. HPLC chromatograms: (a) $\text{TcO}(\text{ox})_2\text{Cl}$ in methanol, approximately 60 min post solution preparation; (b) $\text{TcO}(\text{ox})_2\text{Br}$ in methanol, 15 min post solution preparation.

Table II. Atomic Positional Parameters of Chlorobis(2-methyl-8-quinolinolato)oxotecnium(V)^{a, b}

atom	x	y	z
Tc	0.79842 (5)	0.81763 (3)	0.25108 (3)
Cl	1.0564 (1)	0.8876 (1)	0.15986 (9)
O1	0.6504 (4)	0.9331 (3)	0.1959 (2)
N1	0.5926 (4)	0.7476 (3)	0.3629 (2)
N2	0.7869 (4)	0.6683 (3)	0.1236 (2)
O2	0.8584 (4)	0.9084 (3)	0.3756 (2)
O3	0.9263 (3)	0.6343 (2)	0.3049 (2)
C1	0.4190 (6)	0.6280 (6)	0.2477 (4)
C2	0.4530 (5)	0.6768 (5)	0.3524 (4)
C3	0.3380 (7)	0.6470 (6)	0.4408 (4)
C4	0.3636 (7)	0.6923 (6)	0.5357 (4)
C5	0.5074 (6)	0.7718 (5)	0.5497 (3)
C6	0.6178 (5)	0.7973 (4)	0.4596 (3)
C7	0.7574 (5)	0.8819 (4)	0.4646 (3)
C8	0.7825 (6)	0.9398 (4)	0.5590 (3)
C9	0.6719 (6)	0.9147 (5)	0.6475 (3)
C10	0.5365 (6)	0.8317 (5)	0.6446 (3)
C11	0.6714 (7)	0.8424 (5)	-0.0135 (3)
C12	0.7273 (5)	0.6925 (4)	0.0274 (3)
C13	0.7161 (6)	0.5766 (4)	-0.0371 (3)
C14	0.7653 (5)	0.4383 (4)	-0.0037 (3)
C15	0.8350 (5)	0.4091 (4)	0.0961 (3)
C16	0.8449 (4)	0.5302 (4)	0.1560 (3)
C17	0.9201 (5)	0.5136 (4)	0.2547 (3)
C18	0.9858 (5)	0.3780 (4)	0.2911 (3)
C19	0.9664 (6)	0.2589 (4)	0.2329 (4)
C20	0.8946 (6)	0.2716 (4)	0.1375 (4)

^a The estimated error in the last digit is given in parentheses. This form is used throughout. ^b The numbering scheme is shown in Figure 4.

reaction is a first-order process with a half-life of 1.9 h (Figure 2). The chromatogram of a methanol solution of $\text{TcO}(\text{ox})_2\text{Br}$ at 15-min postmixing (Figure 3) shows essentially only a single peak at the same retention time (8.5 min) as the peak resulting from the chloro analogue. Chromatograms of $\text{TcO}(\text{ox})_2\text{Cl}$ in DMF show a major peak at retention time 6.4 min that does not change significantly over a 24-h period.

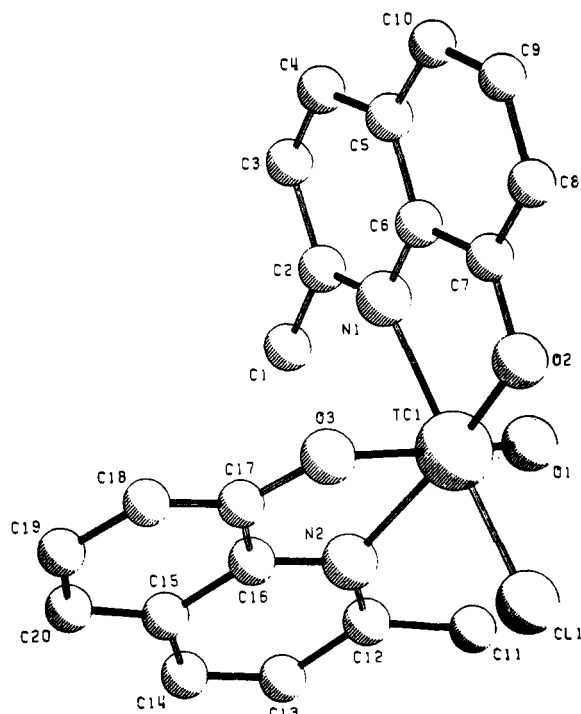
Crystal Structure of Chlorobis(2-methyl-8-quinolinolato)-oxotecnium(V). Final atomic positional parameters are found in Table II; those for hydrogen atoms are listed in Table A.¹⁵ Selected interatomic distances and angles are presented in Table III. Thermal parameters are given in Table B,¹⁵ and the associated ellipsoids are shown in Figures 4 and 5. Observed and calculated structure factors are contained in Table C¹⁵ while a complete listing of bond lengths and angles is

(15) All tables with letter designations have been deposited as supplementary material.

Table III. Selected Bond Lengths and Angles of Chlorobis(2-methyl-8-quinolinolato)oxotechnetium(V)

Bond Lengths, Å			
Tc-Cl	2.360 (1)	Tc-O2	1.947 (3)
Tc-O1	1.649 (3)	Tc-O3	1.994 (3)
Tc-N1	2.179 (3)	O2-C7	1.354 (5)
Tc-N2	2.215 (3)	O3-C17	1.336 (5)

Bond Angles, deg			
Tc-N1-C2	132.8 (3)	N1-Tc-O2	80.7 (1)
Tc-N1-C6	108.1 (2)	N1-Tc-O3	82.1 (1)
Tc-N2-C12	130.4 (3)	N2-Tc-O2	164.2 (1)
Tc-N2-C16	110.8 (2)	N2-Tc-O3	76.2 (1)
Tc-O2-C7	115.6 (2)	O2-Tc-O3	88.5 (1)
Tc-O3-C17	119.5 (2)	Cl-Tc-O1	100.4 (1)
O1-Tc-N1	88.7 (1)	Cl-Tc-N1	168.35 (9)
O1-Tc-N2	90.3 (1)	Cl-Tc-N2	86.42 (8)
O1-Tc-O2	105.4 (1)	Cl-Tc-O2	89.82 (9)
O1-Tc-O3	161.8 (1)	Cl-Tc-O3	90.99 (8)
N1-Tc-N2	100.9 (1)		

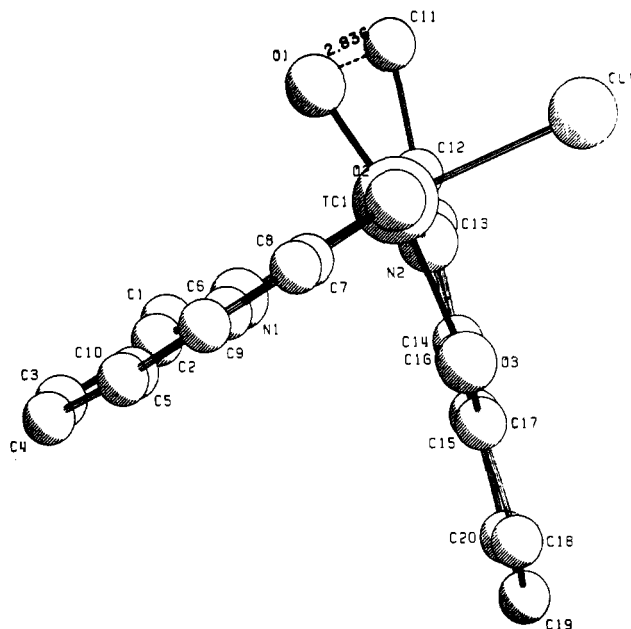
**Figure 4.** PLUTO drawing of $\text{TcO}(\text{oxMe})_2\text{Cl}$ showing structure and atom-labeling scheme.

presented in Tables D and E, respectively.

Discussion

Synthesis, Characterization, and Reactivity. A class of technetium(V) 8-quinolinolates of general formula $\text{cis-TcOL}_2\text{X}$ ($\text{L} = 8\text{-quinolinolate}$; $\text{X} = \text{Cl, Br}$) can be synthesized by simple substitution of the 8-quinolinolate ligand onto TcOX_4^- in methanol. This class of complexes is characterized by the elemental analysis of $\text{TcO}(\text{ox})_2\text{Cl}$, which gives results in agreement with the proposed formulation, by the single-crystal X-ray structural determination of $\text{cis-TcO}(\text{oxMe})_2\text{Cl}$ (vide infra), and by analogous UV-vis and IR spectral parameters of individual complexes (Table I).

In the UV-vis spectra, the magnitude of the molar extinction coefficients indicates that the absorptions are due to charge-transfer transitions. The spectra of the chloro and bromo $\text{TcO}(\text{ox})_2\text{X}$ complexes show no significant differences, and therefore the observed bands do not result from metal-to-halogen or halogen-to-metal charge transfers. However, the λ_{max} of the band near 400 nm does respond to variations in the ox ligand, and thus the charge-transfer process giving rise to this band most likely involves orbitals localized on the 8-quinolinolate ligand.

**Figure 5.** PLUTO drawing of $\text{TcO}(\text{oxMe})_2\text{Cl}$ viewed down the O2-Tc axis, illustrating the close nonbonding contact between O1 and C11 , resulting in repulsion that skews the plane of the N2, O3 oxMe ligand away from O1 and generates an O1-Tc-O3 angle (darkened bonds) of $161.8 (1)^\circ$.

HPLC analysis indicates that in methanol the halide ligand in TcOL_2Cl is susceptible to solvolysis. The time-dependent chromatograms of $\text{TcO}(\text{ox})_2\text{Cl}$ in methanol (Figure 1) show the disappearance of $\text{TcO}(\text{ox})_2\text{Cl}$ and a corresponding increase of a second peak believed to be the product of methanolysis, i.e. $\text{TcO}(\text{ox})_2(\text{OCH}_3)$. This is a relatively slow first-order process, characterized by a specific rate constant of $1 \times 10^{-4} \text{ s}^{-1}$ ($t_{1/2} = 1.9 \text{ h}$) at room temperature, zero ionic strength (Figure 2). HPLC analysis of the bromo analogue $\text{TcO}(\text{ox})_2\text{Br}$ (Figure 3) in methanol shows that within 15 min after solution preparation only a single species is present, and this species exhibits the same retention time as the methanolysis product of the chloro analogue, i.e. $\text{TcO}(\text{ox})_2(\text{OCH}_3)$. This result is reasonable since the bromo ligand is expected to undergo substitution much more rapidly than the chloro ligand, and both $\text{TcO}(\text{ox})_2\text{X}$ complexes should yield the same product upon solvolysis of the halide ligand.

The oxo ligand is known to be a strong labilizing group. For example, in octahedral VO^{2+} complexes the ligands cis to the oxo group undergo substitution with specific rates on the order of 10^{-1} s^{-1} while ligands trans to the oxo group undergo substitution with specific rates greater than 10^7 s^{-1} .¹⁶ The slow rate of methanolysis of $\text{TcO}(\text{ox})_2\text{Cl}$ ($k = 10^{-4} \text{ s}^{-1}$) strongly suggests that the Cl ligand is cis to the trans-labilizing oxo group, and this geometry is indeed confirmed in the X-ray crystal structure of $\text{TcO}(\text{oxMe})_2\text{Cl}$. The rate of methanolysis of $\text{TcO}(\text{ox})_2\text{X}$ is probably controlled by direct substitution of methanol onto the Tc(V) center, rather than by an intramolecular cis to trans isomerization (followed by rapid substitution of the trans-labilized halide) since the bromo complex reacts so much more rapidly than the chloro complex. The geometry of the $\text{TcO}(\text{ox})_2(\text{OCH}_3)$ product has not yet been determined, but there is a possibility that it is a trans isomer since the corresponding complex $\text{trans-TcO}(\text{OCH}_3)(\text{CN})_4^{2-}$ has been reported.¹³

Crystal Structure of Chlorobis(2-methyl-8-quinolinolato)oxotechnetium(V). The structure of $\text{TcO}(\text{oxMe})_2\text{Cl}$ contains discrete molecules without significant intermolecular inter-

Table IV. Structural Parameters for Selected Complexes Containing 8-Quinolinolate^a

complex	N-M-O bite angle, deg	N···O bite dist, Å	M-N, Å	M-O, Å	O-C, Å	N-C(outer), ^b Å	N-C(inner), ^b Å	ref
Cu(ox) ₂	84.5 (6)	2.628 (9)	1.974 (6)	1.935 (6)	1.324 (9)	1.318 (9)	1.351 (9)	} 24
	84.8 (6)	2.628 (9)	1.972 (6)	1.925 (6)	1.317 (9)	1.330 (9)	1.359 (9)	
Zn(ox) ₂	81.5 (6)	2.719 (15)	2.099 (10)	2.066 (10)	1.314 (15)	1.328 (15)	1.342 (15)	25
Pd(ox) ₂ ^c	84.8 (8)	2.675 (30)	1.99 (2)	1.98 (2)	1.31 (3)	1.35 (3)	1.38 (2)	26
Ag(ox)(oxH)	71.7 (2)	2.74 (1)	2.145 (4)	2.505 (5)	1.316 (8)	1.319 (9)	1.401 (8)	} 27
	72.0 (2)	2.72 (1)	2.155 (4)	2.451 (4)	1.325 (7)	1.348 (9)	1.365 (8)	
[Pt(Me) ₃ (ox)] ₂	76 (1)	} NG ^d	2.19 (3)	2.22 (3), 2.29 (4)	1.22 (5)	1.25 (6)	1.33 (5)	} 28
	75 (1)		2.08 (4)	2.22 (4), 2.23 (3)	1.27 (6)	1.37 (6)	1.41 (5)	
TiCl ₃ (ox) ₂	76.9 (6)	2.554 (14)	2.200 (16)	1.888 (11)	1.371 (14)	1.322 (14)	1.350 (12)	29
TcOCl(oxMe) ₂	80.7 (1)	2.677 (4)	2.179 (3)	1.947 (3)	1.354 (5)	1.336 (5)	1.375 (5)	} e
	76.2 (1)	2.603 (4)	2.215 (3)	1.994 (3)	1.336 (5)	1.337 (5)	1.370 (5)	
[MoCl ₃ O(ox)] ⁻	74.5 (2)	2.568 (10)	2.198 (8)	2.039 (5)	1.330 (10)	1.323 (11)	1.369 (10)	19
Mo ₂ O ₃ (ox) ₂ (SCH ₂ CH ₂ O)	76.8 (2)	} NG	2.201 (6)	2.021 (5)	} NG	NG	NG	30
	75.5 (2)		2.209 (6)	2.039 (5)				
[W(NNH ₂)(ox)(PMe ₂ Ph) ₃] ⁺	74.9 (3)	2.605 (10)	2.188 (8)	2.097 (7)	1.331 (12)	1.327 (12)	1.389 (12)	31
[Mo(NNH ₂)(ox)(PMe ₂ Ph) ₃] ⁺	75.6 (1)	2.630 (10)	2.189 (4)	2.102 (3)	1.327 (6)	1.339 (7)	1.379 (6)	31
oxH		2.788 (20)			1.390 (17)	1.350 (17)	1.383 (16)	23
[oxH ₂] ⁺		2.662 (12)			1.360 (11)	1.319 (11)	1.365 (12)	19
[oxH ₂] ⁺ f		2.680 (11)			1.34 (3)	1.32 (3)	1.39 (3)	32

^a Multiple values for individual entries indicate independent ox fragments; ox = 8-quinolinolate; oxMe = 2-methyl-8-quinolinolate. ^b Inner and outer bonds are relative to the center of the ox fragment. ^c Values for this entry were recalculated from atomic positions. ^d NG indicates that the value was not given in the reference. ^e This study. ^f The values quoted here represent the averages of two separate determinations.

actions. Figure 4 illustrates the geometry and atom-numbering scheme. The two methylquinolinolato moieties (hereafter referred to as oxMe) each act as bidentate O,N-donor ligands to the Tc atom that resides in an approximately octahedral coordination environment. One of the oxygen atoms of an oxMe ligand is located trans to the technetium-oxo bond while the remaining three donor atoms of the oxMe ligands plus a chloride ligand occupy the four equatorial sites. The chloride ligand is trans to an oxMe N atom. Distortions from an ideal Tc-centered octahedron are primarily due to the steric requirements of the yl oxygen atom and to the acute bite angles of the oxMe bidentate ligands: 80.7 (1)° for N1-Tc-O2 and 76.2 (1)° for N2-Tc-O3.

The TcO³⁺ core is central to this and many other technetium(V) complexes.^{3,17} The Tc-O1 distance of 1.649 (3) Å indicates multiple-bond character and is typical of Tc=O lengths in complexes where only one such linkage is present (1.65 Å average).¹⁷ The steric requirements of this short bond profoundly distort the stereochemistry of the molecule; particularly significant here is the repulsion within the pairs O1,C1 and O1,O2, evidenced by nonorthogonal angles at Tc of 100.4 (1) and 105.4 (1)°, respectively. Consequently, the Tc atom is displaced 0.22 Å from the mean equatorial plane toward atom O1 (see Table F15).

The O1···C11 nonbonding contact distance (2.836 (5) Å) is remarkably short for an oxo···methyl approach and is much less than the sum of the van der Waals radii of these groups (3.40 Å). This spatial crowding between O1 and the C11 methyl group perturbs the N2,O3-oxMe-Tc bonding; the mean plane of this oxMe ligand is skewed away from the Tc-O1 axis to separate O1 and C11. This perturbation results in (1) the Tc atom lying out of the mean N2,O3-oxMe plane by 0.34 Å, (2) a nonlinear O1-Tc-O3 axis of 161.8 (1)°, and (3) an abnormally long Tc-N2 distance of 2.215 (3) Å. For comparison, other Tc-N(imine) bond distances include 2.179 (3) Å for Tc-N1 in this study, 1.99 (1) Å in [(C₁₂H₁₈O₂N₂)TcO(OH₂)]⁺,¹¹ and 2.087 (5) Å in Tc-(HBPz₃)Cl₂O.¹⁸ Figure 5 clearly shows the O1···C11 contact

and the nonlinear O1-Tc-O3 angle.

The oxo-induced structural trans effect (STE) in molybdenum(V) complexes has been viewed in terms of a steric mechanism where the ligand-ligand repulsions create a cavity larger than necessary for the metal atom.^{19,20} This allows the metal to be displaced out of the mean equatorial plane toward the yl oxygen and elongates the trans bond. This elongation is well documented not only for molybdenum complexes but also for a variety of other metals.²¹ The structural trans effect in TcO(oxMe)₂Cl, calculated as (Tc-O)_{trans} - (Tc-O)_{cis}, is 0.047 (4) Å. The length of (Tc-O)_{trans} (1.994 (3) Å) is in good agreement with (Tc-O)_{trans} in [TcO(dmpe)₂(OH)]²⁺ (1.96 (3) Å) as determined by EXAFS analysis²² and is slightly (~10σ) shorter than the (Mo-O)_{trans} length (2.039 (5) Å) in [MoOCl₃(ox)]⁻.¹⁹

The equatorial coordination environment about Tc also contains interesting bond lengths. The (Tc-O)_{cis} length of 1.947 (3) Å is significantly shorter than the average of single-bonded Tc-O lengths for similar complexes (2.02 Å for Tc(III) or Tc(V), with coordination numbers 6 or 7, not subject to a STE).¹⁷ By this criterion, even the (Tc-O)_{trans} length of 1.994 (3) Å is shorter than expected. Meanwhile, both Tc-N lengths are significantly longer than the "normal" 2.07 Å average.¹⁷ We have speculated (vide supra) that the Tc-N2 bond is lengthened due to steric interference between C11 and O1, and it may be that there exists a synergistic relationship between the long Tc-N2 bond and the short Tc-O2 trans to it. The Tc-C1 length (2.360 (1) Å) is not atypical, 2.34 Å being the average Tc-C1 distance observed

(18) There is another Tc-N bond in Tc(HBPz₃)Cl₂O at 2.26 Å, but it is trans to Tc=O and, thus, subject to a structural trans effect and consequently not relevant to this discussion: Thomas, R. W.; Estes, G. W.; Elder, R. C.; Deutsch, E. *J. Am. Chem. Soc.* **1979**, *101*, 4581.

(19) Yamanouchi, K.; Huenke, J. T.; Enemark, J. H.; Taylor, R. D.; Spence, J. T. *Acta Crystallogr., Sect. B: Struct. Crystallogr. Cryst. Chem.* **1979**, *B35*, 2326.

(20) Garner, C. D.; Hill, L. H.; Mabbs, F. E.; McFadden, D. L.; McPhail, A. T. *J. Chem. Soc., Dalton Trans.* **1977**, 1202.

(21) Shustorovich, E. M.; Porai-Koshits, M. A.; Buslaev, Yu. A. *Coord. Chem. Rev.* **1975**, *17*, 1.

(22) Vanderheyden, J.-L.; Ketring, A. R.; Libson, K.; Heeg, M. J.; Roecker, L.; Motz, P.; Whittle, R.; Elder, R. C.; Deutsch, E. *Inorg. Chem.*, in press.

(17) Bandoli, G.; Mazzi, U.; Roncari, E.; Deutsch, E. *Coord. Chem. Rev.* **1982**, *44*, 191.

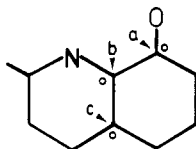


Figure 6. Upon coordination of 2-methyl-8-quinolinolate to Tc, the angles indicated by arrows are contracted from the ideal 120° value, while the angles identified with circles are concomitantly greater than 120° . Values for angles a - c in the two $[\text{oxMe}]^-$ ligands are 118.7 , 116.9 , and 116.1° for N1 oxMe and 116.2 , 115.9 , and 115.9° for N2,O3 oxMe.

in similar complexes¹⁷ and $2.358(3) \text{ \AA}$ being reported for Mo-C1 (trans to the N of the 8-quinolinolate (ox) ligand in $[\text{MoOCl}_3(\text{ox})]^-$).¹⁹

This structure presents an opportunity to observe the coordinated 2-methyl-8-quinolinolate ligand in two perpendicular environments relative to a Tc=O bond. The steric repulsion between O1 and C11 induces considerably more strain within the N2,O3-oxMe ligand (relative to the N1,O2-oxMe ligand) as evidenced by (1) the O-Tc-N bite angle being smaller for N2,O3-oxMe ($76.2(1)^\circ$) than for N1,O2-oxMe ($80.7(1)^\circ$), (2) the N...O bite distance also being smaller for N2,O3-oxMe ($2.603(4) \text{ \AA}$) than for N1,O2-oxMe ($2.677(4) \text{ \AA}$), (3) N2,O3-oxMe being significantly more strained at key internal angles (see Figure 5). It should be noted that both oxMe ligands show bite distances significantly smaller than that of the free neutral molecule ($2.788(20) \text{ \AA}$).²³

Assembled in Table IV are some structural parameters of complexes containing 8-quinolinol (ox) fragments. Although it is difficult to compare structures containing different metal ions, there are certain obvious trends that emerge from examination of these parameters. Larger N-M-O bite angles ($>81^\circ$) are all associated with structures in which pairs of ox ligands are arranged in a square-planar geometry, i.e. in Cu(ox),²⁴ Zn(ox),²⁵ and Pd(ox).²⁶ The N...O bite distance is

largest for the free neutral molecule ($2.788(20) \text{ \AA}$),²³ while all other species, including the protonated cation $[\text{oxH}_2]^+$, show some degree of contraction from this resting value. Overall, the M-N distance is significantly longer than the M-O distance whenever the oxygen atom is not additionally coordinated. Those structures with bridging O(ox) atoms exhibit longer than usual M-O bonds and are $\text{Ag}(\text{ox})(\text{oxH})$,²⁷ in which oxygen atoms from ox ligands of adjacent molecules are bridged by a H^+ ion, and dimeric $[\text{Pt}(\text{Me})_3(\text{ox})]_2$,²⁸ in which the two Pt atoms are doubly bridged by the oxygen atoms of the ox ligands. From Table IV it is also seen that within a group of similarly sized metals, the O-C length generally varies inversely with the M-C distance. Variations in bonding radii for these metals and variations in the esd's prohibit a quantitative assessment, but the trend is clearly evident. In reference to the N-C bond lengths in these 8-quinolinolate structures, without exception we see that the N-C (outer) length is shorter than the N-C (inner) length, where inner and outer are relative to the center of the ox fragment; we assume that this effect is electronic and characteristic of ox molecules in general.

Acknowledgment. Financial support by the National Institutes of Health (Grant No. HL-21276) is gratefully acknowledged.

Registry No. TcO(ox)₂Cl, 91281-87-7; TcO(ox)₂Br, 91281-88-8; TcO(oxCl₂)₂Cl, 91281-89-9; TcO(oxBr₂)₂Cl, 91281-90-2; TcO(oxMe)₂Cl, 91281-91-3; TcO(oxNO₂)₂Cl, 91281-92-4; $[\text{Bu}_4\text{N}]\text{TcOCl}_4$, 71341-65-6; $[\text{Bu}_4\text{N}]\text{TcOBr}_4$, 73953-03-4.

Supplementary Material Available: Tables of hydrogen positional parameters (Table A), anisotropic thermal parameters (Table B), observed and calculated structure factors (Table C), bond lengths (Table D), bond angles (Table E), and least-squares planes (Table F) for TcO(C₁₀H₈NO)₂Cl (18 pages). Ordering information is given on any current masthead page.

- (23) Roychowdhury, P.; Das, B. N.; Basak, B. S. *Acta Crystallogr., Sect. B: Struct. Crystallogr. Cryst. Chem.* **1978**, *B34*, 1047.
 (24) Palenik, G. J. *Acta Crystallogr.* **1964**, *17*, 687.
 (25) Palenik, G. J. *Acta Crystallogr.* **1964**, *17*, 696.
 (26) Kamenar, B.; Prout, C. K.; Wright, J. D. *J. Chem. Soc.* **1965**, 4851.

- (27) Fleming, J. E.; Lynton, H. *Can. J. Chem.* **1968**, *46*, 471.
 (28) Lydon, J. E.; Truter, M. R. *J. Chem. Soc.* **1965**, 6899.
 (29) Studd, B. F.; Swallow, A. G. *J. Chem. Soc. A* **1968**, 1961.
 (30) Gelder, J. I.; Enemark, J. H.; Wolterman, G.; Boston, D. A.; Haight, G. P. *J. Am. Chem. Soc.* **1975**, *97*, 1616.
 (31) Hanson, I. R.; Hughes, D. L. *J. Chem. Soc., Dalton Trans.* **1981**, 390.
 (32) Ruzic-Toros, Z.; Kojic-Prodic, B.; Gabela, F.; Sljukic, M. *Acta Crystallogr., Sect. B: Struct. Crystallogr. Cryst. Chem.* **1977**, *B33*, 692.